



P-230

Application of Common Offset Inversion Over Geological Models

Shikher Shishodia*, IIT Roorkee

Summary

Seismic representation of an earth model in depth is usually described by two sets of parameters – layer velocities and reflector geometries. Nearly all of the practical methods of layer velocity and depth estimation are based on ray theory, and more specifically on inversion of seismic travel time. In trying to resolve complex geological structures, the pitfalls in employing the CDP method become evident. Additionally, stacking of multi-offset traces corrupts the amplitude necessary for stratigraphic analysis. In order to preserve whatever structural and amplitude information is in the data, pre stack inversion should be performed. Given common offset data and velocity above the reflector, pre stack acoustic Kirchhoff inversion resolves the location of the interfaces.

In this work, an attempt has been made to generate geological models and later smoothen by damped least square technique. On the basis of above models, synthetic common offset seismic sections are generated. These common offset seismic sections are further inverted and corresponding offset-depth models are obtained.

Keywords: Velocity smoothening technique, 3D inversion operator and 2.5 D inversion operator

Introduction

In exploration for hydrocarbons, the areas of greatest interest are those where the geology is the most complicated. As the complexity of the subsurface increases, the validity of stacking and poststack processing decreases. In these cases, reflector location and velocity information must be recovered prior to stacking. To accomplish this, an inversion method is needed for common-shot, common-receiver, or common-offset time records. In all acquisition geometries, reflection coefficients occur at non-normal incidence. Inversion therefore yields reflection coefficients as a function of incident angle. Common offset data shows less angular variation of the reflection coefficients. The larger the data collection zone, the greater the delineated portion of the subsurface. In general, common-offset data dictate less angular variation of the reflection coefficient since the separation between source and receiver is fixed at the same distance for each experiment (Sullivan and Cohen, 1987). Since the following theory is based on the acoustic wave equation and is to be applied to an elastic world, angles associated with large offsets are to be avoided. Another important consideration in the selection of an inversion data set is the acquisition area of the surface. The larger the data collection zone, the

greater the delineated portion of the subsurface. High frequency. Constant-density, Kirchhoff offset modeling for a single arbitrary surface provides the basis of the following inversion (Sullivan and Cohen, 1987). Given the compressional wave speed of the first medium, the Kirchhoff wave-field effects are inverted to yield the location of the interface and the angularly dependent reflection coefficient at each point on the interface.

Theory

Velocity smoothening technique

Velocity smoothening is helpful in reducing the inversion error due to high frequency assumptions and calculations. A smoothening process can be viewed as an averaging process over a specific range (Liu, 1994). Damped least square (DLS) method is one of the best approaches in order to suppress the lateral velocity variation derivative for a layered earth. Compared to the convolution type approach, computational time of the DLS method is independent of the smoothening operator length (Liu, 1994).

In Damped least square method, a smooth velocity function is sought that minimizes the weighted sum of,



- i. The deviation between the smooth velocity and the original one.
- ii. The first derivatives of the velocity.

This minimization problem is equivalent to the second order differential equation which can be solved very efficiently. With the help of iterative feature DLS method can suppress higher order derivatives to satisfy various purposes. Unlike to the other method computational cost is independent of the length of the parameter, therefore, DLS will work if the velocity smoothening requires a long smoothening operator (Liu,1994). DLS can handle a local velocity variation in the degree of velocity smoothening so that the smoothening factor can be achieved with high degree of accuracy.

In the DLS method, the smoothed velocity $v_s(x)$ is determined by the equation,

$$\int \omega(x)(v_s(x)-v(x))^2 dx + \alpha^2 \int (dv_s/dx)^2 dx = \min \quad (1)$$

α - smoothening parameter and $w(x)$ is weighting function, ranging from 0 to 1. This weighting function can be defined by,

$$\omega(x) = 1/(1+x^2\mu^2) \quad (2)$$

Where x is depth and μ is constant. The larger value of μ the faster the $w(x)$ decreases with depth. The equivalent differential form of minimization (1) is given by

$$\omega(x)v_s(x) - \alpha^2(d^2v/dx^2) = \omega(x)v(x) \quad (3)$$

In discretization, the above differential equation becomes a tridiagonal linear system that can be solved very efficiently. Minimization (1) smoothes a velocity by suppressing its first derivative. Generally, the smoothening will be better if higher order derivatives are suppressed. Thus one general formula for all higher order derivatives can be given as,

$$\omega(x)v_n(x) - \alpha^2(d^2v_n/dx^2) = \omega(x)v_{n-1}(x) \quad (4)$$

Where $n= 1,2,3,\dots$

$$v_n(k) = v_{n-1}(k) / (1+\alpha^2k^2) \quad (5)$$

where v_n and v_{n-1} are Fourier transforms of v_n and v_{n-1}

respectively.

Repeating equation (3) for n times

$$V_n(k) = v(k)(1+\alpha^2k^2)^{-n} \quad (6)$$

Therefore large wave number components in the smoothed velocity component is suppressed.

Using the length of a smoothing operator allows to chose a smoothing parameter avoiding to the range over which the original velocity required to be averaged. where V is the Fourier transform of V .

The figures 1(b),2(b),3(b) show the smoothed velocity model of different geological structures after application of Damped Least Square method. It can be easily inferred from the figures that applied velocity variation (Lateral as well as vertical) are suppressed in a great amount. This smoothed velocity model is input for Kirchhoff's forward modeling.

Generation of Kirchhoff's forward model

In order to simulate and invert pre-stack data, a forward modeling procedure is required. The Kirchhoff integral method is chosen since it is embedded in wave theory and, as such, produces wave-field effects (Bleistein,1986) The development presented here is suited to the modeling of common-source, common-receiver, or common-offset gathers. Of particular interest to the inversion of the next section are data acquired with a constant offset between the source and receiver.

An assumption of high-frequency data underlies both the forward modeling and the inversion theory. The choice of a suitably high frequency is a function of both a distance parameter and the velocity of the medium (Bleistein, Cohen and Hagin,1987). By assuming that all frequencies in the data are greater than this minimum high frequency. Asymptotic evaluations are justified. The distance parameter 'r' may be the minimum depth to an interface or a radius of curvature for a reflector. To provide a reasonable approximation, the following relationship must be satisfied,

$$2\omega r/c \gg 1$$



where the 2 corresponds to the two-way travel time of the forward or inverse problem. For example, if the depth to the reflector is 152 m in a medium with a compressional wave speed of 3 048 m/s, any frequency above 5 Hz is suitable since the amplitude error at the low end (5 Hz) of the frequency spectrum is only a few percent.

The subsequent derivation yields the high-frequency Kirchhoff representation of the wave field reflected from an arbitrary surface. In each experiment the source is offset from the receiver. For modeling purposes. This experiment is repeated along the surface to generate a time section of common-offset traces.

The scattered field from the reflector is governed by the homogeneous wave equation

$$\nabla^2 U_s(\omega, r, r^+) + (\omega^2/c^2)U_s(\omega, r, r^+) = 0 \quad (7)$$

The two spatial variables of the argument of KJ, in equation (7) indicate that the recorded value of the scattered field U_s at any point r is a function of the source position r^+ . Since the scattered field is recorded at only one receiver location r^- per experiment, a sifting operation is necessary on the variable r of equation (7).

For the purpose of sifting under a volume integral, a second wave equation is introduced:

$$\nabla^2 g(\omega, r, r^-) + (\omega^2/c^2)g(\omega, r, r^-) = -\delta(r-r^-) \quad (8)$$

The solution $y(\omega, r, r^-)$ is a free-space Green's function which describes the propagation of a point source from the location r^- toward any point r . Employing reciprocity to interchange r and r^- and applying Green's theorem to the two wave equations yields

$$U_s(\omega, r^-, r^+) = \iint ds [U_s(\omega, r, r^+) \frac{\partial g(\omega, r, r^-)}{\partial n} - g(\omega, r, r^-) \frac{\partial U_s(\omega, r, r^+)}{\partial n}] \quad (9)$$

where the unit normal vector \mathbf{n} is pointing inward, and the closed surface is composed of the reflector truncated at its intersection by a large hemisphere having its base on the reflector.

To compute $U_s(\omega, r^-, r^+)$, the scattered field and its normal Derivative on the reflector are needed. An

approximate solution for the scattered field near the reflector, due to an incident point source, has the following form:

$$U_s(\omega, r, r^+) = R \cdot \exp(i\omega/c|r-r^+|)/4\pi|r-r^+| \quad (10)$$

$$R = (\gamma_i - \gamma_t)/(\gamma_i + \gamma_t) \quad (11)$$

$$\text{Where } \gamma_i = \mathbf{n} \cdot |\mathbf{r}-\mathbf{r}^+|/c \quad (12)$$

$$\text{And } \gamma_t = \text{sgn}(c_i^2 - c^2 + \gamma_i^2)^{1/2} \quad (13)$$

Where c and c_1 are the velocities above and below the reflector, respectively.

The high frequency approximation of the normal derivative is approximated by

$$\frac{\partial g(\omega, r, r^-)}{\partial n} = \frac{\exp\left[\left(\frac{i\omega}{c}\right)|r^- - r|\right] \times \left(\frac{i\omega}{c}\right)(\nabla|r^- - r|\mathbf{n})}{4\pi|r^- - r|} \quad (14)$$

Combining all these approximation, total scattered field can be written as

$$U_s(\omega, r^-, r^+) = \frac{i\omega}{16\pi^2} \iint ds R[\gamma^+ + \gamma^-] \times \exp\left[\frac{\left(\frac{i\omega}{c}\right)(|r-r^+|+|r^- - r|)}{|r-r^+||r^- - r|}\right] \quad (15)$$

Equation (15) provides a high-frequency Kirchhoff wave-field response for non-zero offset modeling.

Applying this forward modeling(8s)scheme on the previous considered Models the common offset time section is shown in figure 1(c),2(c),3(c). Here the offset is taken as 100m. Here the record length is taken as 2 second to incorporate all the events.

The common offset section clearly outlines the anticline structure. At the position of edges diffraction hyperbolae are present.

Application of two and one half dimension Born inversion

In this work two and one half dimensional Born inversion is applied on common offset data.2.5D approximation retains the 3D point source model.

3D Inversion operator

In the forward problem, each trace is viewed as weighted



sum of the image sources on a reflector. Therefore inversion of forward data to determine the interface location must involve a weighted sum of recorded surface traces. Also an inverse phase term is related to inversion as wave is propagating back to surface (Lambar et.al, 2003)

3D inversion operator is given by

$$W[U(\omega, m)] = \iint dm^2 \int d\omega(-i\omega) \times \exp\left[\left(-\frac{i\omega}{c}\right)(R'^+ + R'^-)\right] U(\omega, m) \quad (16)$$

The frequency-domain version of the input data is represented by $U_s(\omega, m)$, with the vector 'm' parameterizing the midpoint associated with each experiment, R'^+ is the distance between the source and the test point, and R'^- is the distance from the test point to the receiver.

Considering all this parameter, general 3D Kirchhoff pre-stack inversion formula is given by,

$$W[U(\omega, m)] = \iint dm^2 \int d\omega \times \exp\left[\left(-\frac{i\omega}{c}\right)(R'^+ + R'^-)\right] U_s(\omega, m) n \times \frac{(R'^+ + R'^-)(R'^+ + R'^-)}{(R'^+ \times R'^-)} \sqrt{2(1 - R'^+ \times R'^-)} \quad (17)$$

The singular function acts when the test point is on the reflector R^+ is then replaced by R'^+ . The location of the interface is therefore determined by employing equation (17) on common offset data.

2.5 D inversion operator specialization

The 2.5D Kirchhoff common offset inversion operator is given by

$$W[U_z(\omega, m_1)] = \frac{-2z}{\pi^2} \int dm_1 \int |\omega|^{\frac{1}{2}} d\omega \times \frac{(R'^+ + R'^-)^{-\frac{1}{2}}}{(R'^+ R'^-)^{\frac{3}{2}}} (R'^+ + R'^-)^2 \sqrt{1 - R'^+ R'^-} \times \exp\left[\left(-\frac{i\omega}{c}\right)(R'^+ + R'^-)(i3\pi/4)\right] U_z(\omega, m_1)$$

Where R^+ and R^+ are evaluated at stationary points.

In this work, 2.5D inversion scheme is applied on the prestack common offset data. The inversion is applied for each 5th skipped midpoint and final result is interpolated by 'upper triangulation method'. The inverted section is given in the figure 1(d), 2(d),3(d).

Conclusions

- i. Lateral velocity variation can be easily taken care by this method. DLS is efficient to suppress second order or higher order horizontal velocity derivatives. Here only the first order derivatives have been considered .thus DLS is fruitful technique in prestack common offset inversion.
- ii. Fault planes can be easily distinguished by discontinuity at the edges of reflectors.
- iii. However the edges of the reflectors are not delineated properly and some numerical artifacts have been observed at the edges. These may be the result of over estimation of background velocities, error due to inversion and wrong approximation of slowness perturbation.
- iv. Numerical artifacts in the inverted section increases as depth increases.It is quite visible that these artifacts are comparatively more in the last horizontal interface than the first interface of model2 and model3.
- v. One of the major drawbacks of this method is that it does not recover the velocity profiles of the layers.



Appendix

MODEL 1 : Anticline

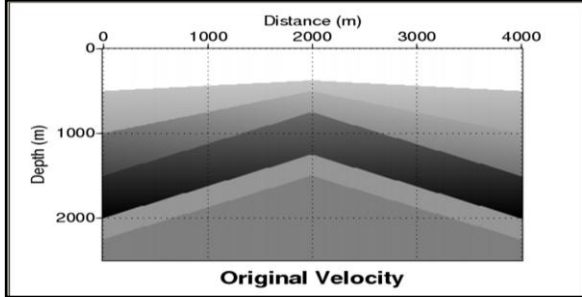


Figure 1(a)

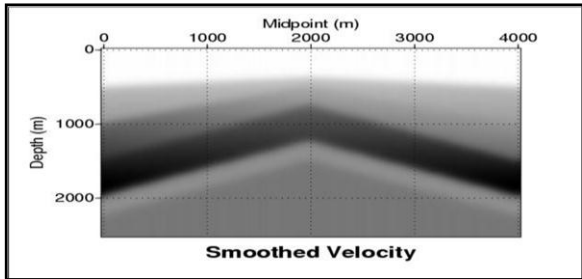


Figure 1(b)

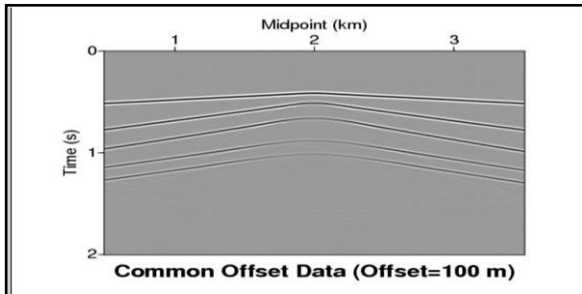


Figure 1(c)

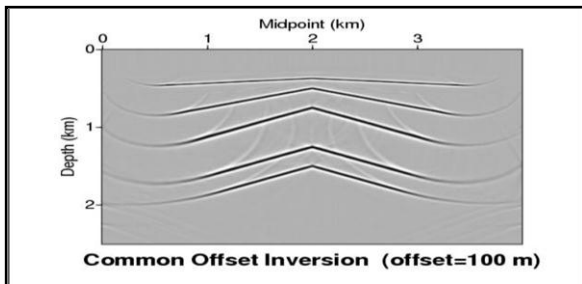


Figure 1(d)

MODEL 2 : Antisyncline

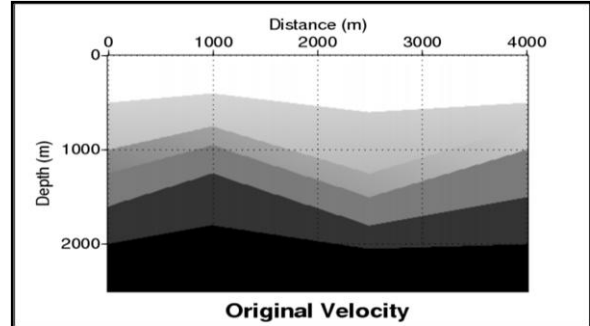


Figure 2(a)

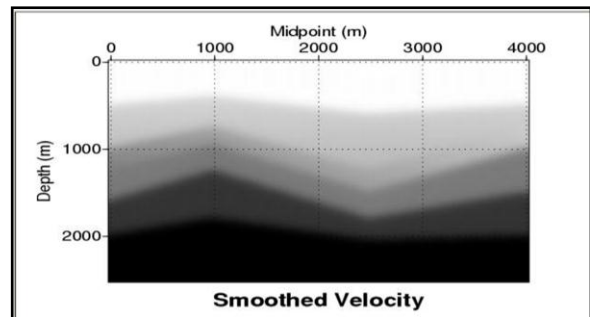


Figure 2(b)

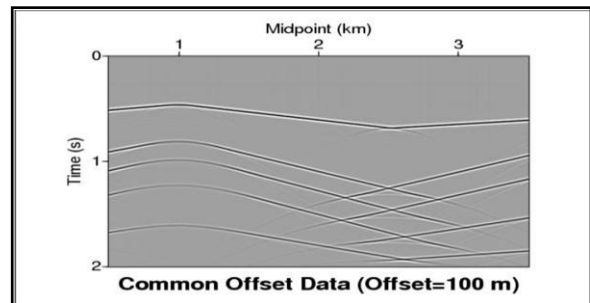


Figure 2(c)

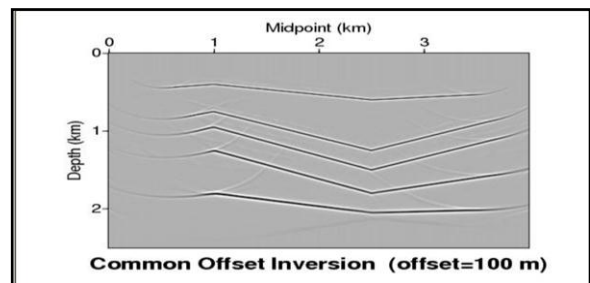


Figure 2(d)



MODEL 3: Salt dome

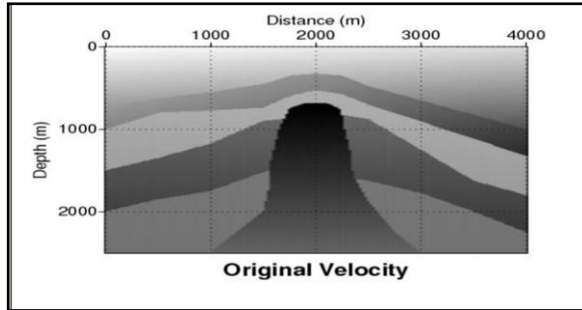


Figure 3(a)

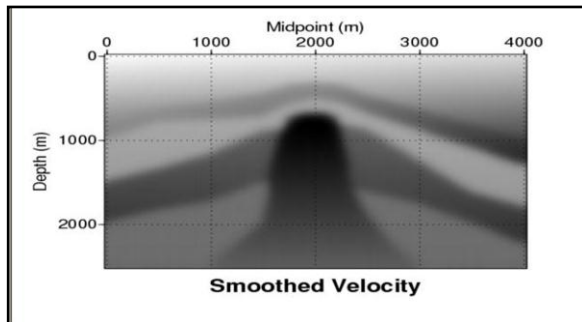


Figure 3(b)

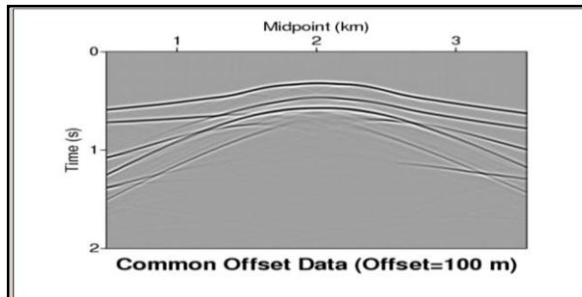


Figure 3(c)

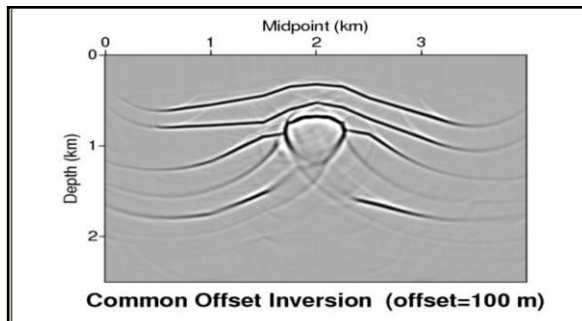


Figure 3(d)

References

Bleistein, N., 1986, Two-and-one-half dimensional in-plane wave propagation: *Geophys. Prosp.*, 34, PP.686-703

Bleistein, N., Cohen, J. K., and Hagin, F. G., 1987, Two-and-one-half dimensional Born inversion with an arbitrary reference: *Geophysics*, 52, 26, 36.

Lambar, G.; Operatoz, s; Podvin, P; and Thierry, p; 2003, 3D ray+Born migration/inversion-part 1: *Theor. Geophysics*, 68, PP.1348-1356

Liu, Z; 1994, A velocity smoothening technique based on Damped least squares: in project review, consortium project on Seismic Inverse Methods for Complex Structures, CWP-153

SEISMIC UNIX Manual, 2002, center of wave phenomena (CWP), Colorado School Of Mines, U.S.A

Sullivan, M. F., and Cohen, J. K., 1987, Pre-stack Kirchhoff inversion of common offset data, *Geophysics*, 52, PP.745-754

List of figures

- Figure 1(a) Original Velocity-Depth Models (Anticline)
- Figure 1(b) Smoothed Velocity Model
- Figure 1(c) Common Offset Time Section
- Figure 1(d) Common Offset Inverted Section (Offset=100m)
- Figure 2(a) Original Velocity-Depth Models (Anti-Syncline)
- Figure 2(b) Smoothed Velocity Model
- Figure 2(c) Common Offset Time Section
- Figure 2(d) Common Offset Inverted Section (Offset=100m)
- Figure 3(a) Original Velocity-Depth Models (Salt dome)
- Figure 3(b) Smoothed Velocity Model
- Figure 3(c) Common Offset Time Section
- Figure 3(d) Common Offset Inverted Section